Orthogonal Wavelet Analysis of Flow Structures in Asymmetric Wakes

Shun FUJIMOTO and Akira RINOSHIKA
Department of Mechanical Systems Engineering, Graduate School of Science and Engineering, Yamagata University, Yamagata, 992-8510, Japan

Keywords: Vorticity, Turbulent wake, Flow visualization, Orthogonal wavelet transform, Reynolds stress

1. Introduction

The turbulent near wake generated by a bluff body has caused the aerodynamic drag, vibration and noise. Therefore, when designing the vehicle body, aero-plane wing and so on, it is very important to study wake structures and to control wake flow. In the past decade, there has been a growing interest in applying the wavelet technique to the analysis of turbulent flow data. This technique allows time- or spatial- and frequency-domain analyses to be combined and decomposes the flow structures based on frequencies or scales. Recently, Rinoshika and Zhou [1-3] developed a one-dimensional orthogonal wavelet multi-resolution technique to analyze the hot-wire data for studying the turbulent structures of different scales in the near and far wakes of circular cylinder and screen cylinder. Using the high-speed PIV technique, Rinoshika and Omori [4] also investigated the turbulent structures of various scales on square and compound cylinders.

In this study, turbulent wake structures of various scales generated by asymmetric body were experimentally measured by the high-speed PIV. Then one- and two-dimensional wavelet multi-resolution technique was used to analyze the instantaneous velocity and vorticity measured by PIV technique in the circulating water channel, and turbulent structures were decomposed into a number of subsets based on their central frequencies, which are linked with the turbulent scales. Reynolds stress and vorticity of various frequencies were examined.

2. Experimental Details

Experimental asymmetric bluff body and the experimental setup were shown in Fig.1. Experimental model of wake generator has a scale of L = 50 mm. The experiment was conducted in the circulating water channel, which has a 400 mm × 200 mm × 1000 mm working section. Tracer particles 63 ~ 75 μm in diameter were seeded in the flow loop of circulating water channel. By the use of laser light sheet and high-speed camera (Photoron FASTCAM SA3), the digital images were captured at frame rate of 500 fps and the shutter speed of 1 ms. 1025 images were analyzed by PIV software. The high-speed PIV measurements were carried out at a constant velocity of U = 0.19 m/s, corresponding to Re ($\equiv UL/\nu$) = 8960.

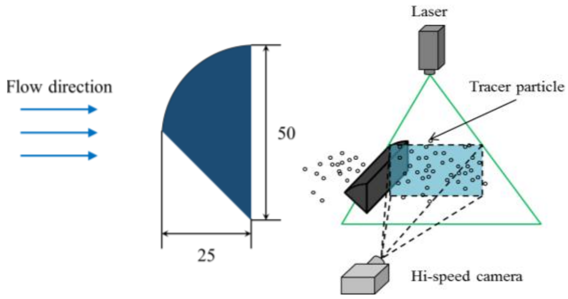

Fig.1 Experimental setup and model.

3. Orthogonal Wavelet Transform Algorithm

In this study, the discrete data are decomposed into a number of wavelet components based on characteristic frequencies by orthogonal wavelet multi-resolution technique. One-dimensional orthogonal wavelet multi-resolution technique is first used to analyze fluctuation velocities and Reynolds shear stresses of various scales are evaluated. Then two-dimensional orthogonal wavelet multi-resolution technique is used to analyze vorticity.

As an example, one-dimensional wavelet multi-resolution technique is briefly described in this section. One-dimensional wavelet transform is defined in matrix form by

$$\boldsymbol{S} = \boldsymbol{W}\boldsymbol{X} \tag{1}$$

where $\boldsymbol{X}$ is one-dimensional data matrix, namely,

$$\boldsymbol{X} = [\boldsymbol{x}_1 \quad \boldsymbol{x}_2 \quad \ldots \quad \boldsymbol{x}_N]^T \tag{2}$$

The superscript T indicates a transposed matrix. $\boldsymbol{S}$ and $\boldsymbol{W}$ are called the orthogonal wavelet coefficient matrix and the analyzing wavelet matrix, respectively. $\boldsymbol{W}$ is orthogonal and satisfies,

$$\boldsymbol{W}^T\boldsymbol{W} = \boldsymbol{I} \tag{3}$$

where $\boldsymbol{I}$ is an unit matrix. Therefore, the discrete wavelet transform is the inverse wavelet transform, which is given by

$$\boldsymbol{X} = \boldsymbol{W}^T\boldsymbol{S} \tag{4}$$

In order to decompose the data into the grouped frequency components, the inverse wavelet transform is applied to the discrete wavelet coefficients at each grouped frequency. This decomposition method is called the wavelet multi-resolution analysis and can be written as

$$\boldsymbol{X} = \boldsymbol{W}^T\boldsymbol{S}_1 + \boldsymbol{W}^T\boldsymbol{S}_2 + \cdots + \boldsymbol{W}^T\boldsymbol{S}_N \tag{5}$$

The remarkable point doesn't contain redundant information. In this study, the Daubechies wavelet matrix with an order of 12 is used as the analyzing wavelet matrix.

4. Results and Discussion

Figure 2 shows instantaneous streamlines and corresponding normalized vorticity contour in the (x, y)-plane. The color mappings have been assigned to the vorticity values and the highest concentration is displayed as red and the lowest as blue, respectively. The asymmetric large-scale vortices shed from body are clearly observed.

Figure 3 presents the Reynolds shear stress contours calculated from the wavelet components of the instantaneous velocity at wavelet levels 1 and 5 in the (x, y)-plane. It is evident that Reynolds shear stress of level 1 exhibit the maximum values near the end of the separation region, corresponding well to the measured Reynolds shear stress contour. It indicates that the most significant contribution to the Reynolds shear stress comes from the large-scale structures. When decreasing the scale of structures to level 5, the region of the maximum Reynolds shear stress appears near the asymmetric body and the separation shear layer. It indicates that the relatively small-scale structure dominates this region.

Figure 4 shows the streamlines and vorticity contours of the wavelet components at level 1 and level 2 in the (x, y)-plane. The streamlines and vorticity contours at level 1 coincide approximately with the measured data of Fig.2, implying the large-scale structures make the most contribution to flow structure. As decreasing the scale of structures to level 2, relatively small-scale structures are observed in all flow field.

References

1) A. Rinoshika and Y. Zhou, Orthogonal Wavelet Multi-Resolution Analysis of a Turbulent Cylinder Wake, *J. Fluid Mech.* **524**(2005) 229-248.
2) A. Rinoshika and Y. Zhou, Effects of Initial Conditions on a Wavelet-decomposed Turbulent Near-wake, *Physical Review E* **71**(2005) 046303 1-8.
3) A. Rinoshika and Y. Zhou, Reynolds Number Effects on Wavelet Components of Self-preserving Turbulent Structures, *Physical Review E* **79**(2009) 046332 1-11.
4) A. Rinoshika and H. Omori, Orthogonal wavelet analysis of turbulent wakes behind various bluff bodies, *Experimental Thermal and Fluid Science* **35**(2011) 1231-1238.

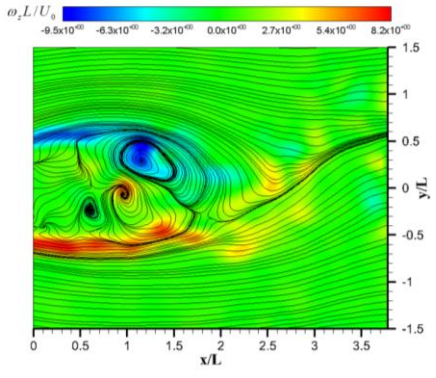

Fig.2 Instantaneous streamlines and corresponding normalized vorticity contours in the (x, y)-plane.

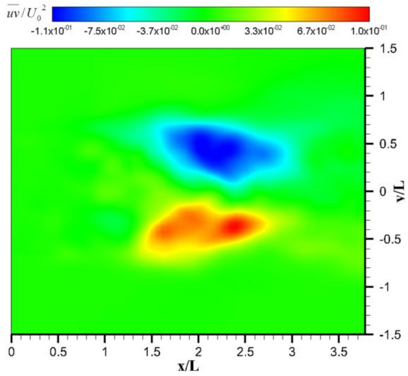

(a) level 1

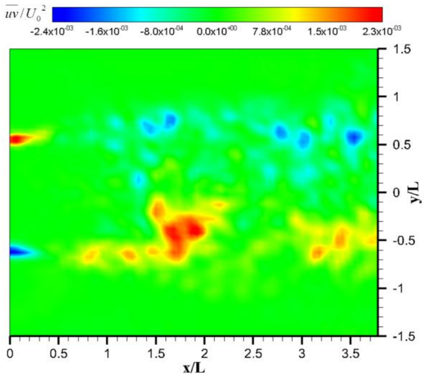

(b) level 5

Fig.3 Reynolds shear stress contours of wavelet components in the (x, y)-plane.

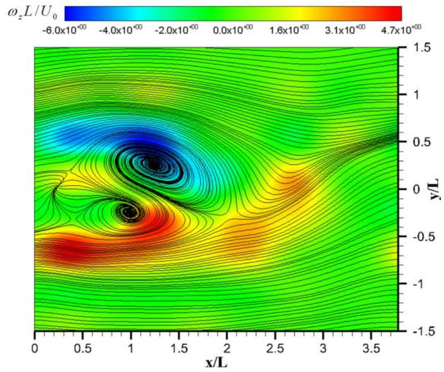

(a) level 1

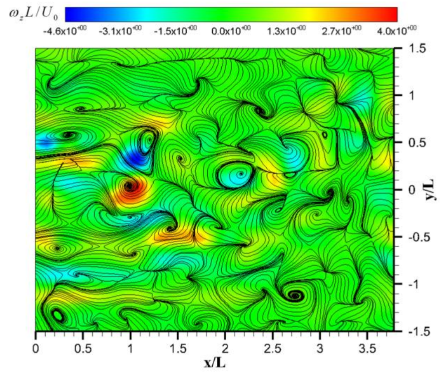

(b) level 2

Fig.4 Streamlines and vorticity contours of the wavelet components in the (x, y)-plane.